Robust QoS-Constrained Optimization of Downlink Multiuser MISO Systems

Nikola Vučić, *Student Member, IEEE,* and Holger Boche, *Senior Member, IEEE*

***Abstract*—The knowledge of the channel at the transmit side of a communication system can be exploited by using precoding techniques, from which the overall transmission quality might benefit significantly. However, in practical wireless systems, the channel state information is prone to errors, which sometimes deteriorates the performance drastically. In this paper, we address the problem of robust transceiver design in a downlink multiuser system, with respect to the erroneous channel knowledge at the transmitter. The base station is equipped with an antenna array, while users have single antennas. The transceiver optimization is performed under a set of predefined users' quality-of-service constraints, defined as maximum mean square errors, or minimum signal-to-interference-plus-noise ratios, which must be satisfied for all disturbances that belong to given, bounded uncertainty sets. Efficient numerical solutions are obtained using semidefinite programming methods from convex optimization theory. The proposed algorithms are found to outperform related approaches in the literature in terms of the achieved performance, while maintaining low computational complexity. The studied uncertainty models are applicable in mitigating typical errors that emerge as a result of quantization or channel estimation.**

***Index Terms*—Multiuser multiple-input single-output (MISO) systems, joint transmit-receive equalization, robustness, semidefinite programming, ellipsoid method.**

I. Introduction

The ability to exploit the spatial diversity by employing antenna arrays and provide significant performance gains has given a great stimulus in wireless communications research in recent years [1]. Systems in which a multi-antenna base station (BS) serves single-antenna users present promising candidates for future cellular networks, since the complex signal processing is performed at the BS, where the issue of computational power is less problematic, while the mobile units can be kept relatively simple and inexpensive.

In the downlink of such setups, which is a multiuser multiple-input, single-output (MISO) scenario, precoding methods can be applied to boost the performance. The idea is to pre-equalize signals at the transmitter, and mitigate the channel-induced interference [2]. These techniques naturally demand that the channel state information (CSI) is supplied at the transmit side. However, the provision of *perfect* CSI is often a formidable task in wireless systems. The transmitter typically obtains the channel knowledge either through feedback channels from the receiver, where it is estimated using training sequences, or by estimating it in the uplink phase directly, with the latter approach being applicable in time division duplex (TDD) systems. In both cases, estimation errors are inevitable in practice [3]. Furthermore, the feedback channels are usually of limited capacity [4], so the quantization effects must be taken into account. If the uplink values are used, the problem of having outdated estimates appears frequently, because of the fast varying wireless environment. These effects, along with the fact that the downlink precoding methods can be quite sensitive to the imperfect CSI [5], instigated a significant amount of research work in enabling a sort of robustness regarding the channel knowledge. Considered robust designs are usually either of stochastic or the worst-case nature.

Stochastic robustness has been studied in [6]–[11], assuming that the error in the channel knowledge possesses certain statistical properties. This hypothesis is in some cases reasonable, since the error in the estimation process can often be approximated as a random variable with the Gaussian distribution. Statistical assumption on the CSI disturbance can then be used for optimizing the mean or the outage performance of the system. A related direction in probabilistic approaches is the transmitter design under the assumption of having only statistical properties of the exact channel, like the mean or the covariance of the channel coefficients (see, e.g., [12], [13]).

Worst-case analysis, that we adhere to in this paper, is also well-established in robust signal processing [9], [10], [14]–[19]. Here, the errors are supposed to belong to the given bounded uncertainty sets, and the system is optimized to satisfy certain requirements for all channels from the uncertainty regions. This approach requires no statistical assumption on the disturbances, which often indeed do not exhibit any, and corresponds well to the quantization errors. It is also convenient for handling slow fading channels, where no sufficient statistics for the averaging is available [20]. The robustness against unbounded errors (e.g., the ones with the Gaussian distribution) can also be supported with this model by controlling the system outage [18].

The main problem of interest in this paper is the transceiver optimization with the goal of minimizing the total transmit

N. Vučić is with the Fraunhofer Institute for Telecommunications - Heinrich Hertz Institute, Berlin, Germany (e-mail: nikola.vucic@hhi.fraunhofer.de).

H. Boche is with the Technical University Berlin - Heinrich Hertz Chair for Mobile Communications, Berlin, Germany. He is also with the Fraunhofer Institute for Telecommunications - Heinrich Hertz Institute and with the Fraunhofer German-Sino Mobile Communications Lab, Berlin, Germany (e-mail: holger.boche@mk.tu-berlin.de).

This work is supported by the STREP project No. IST-026905 (MASCOT) within the sixth framework programme of the European Commission. Parts of this work were presented at the International Workshop on Computational Advances in Multi-Sensor Adaptive Processing (CAMSAP 2007), St. Thomas, U.S. Virgin Islands, Dec. 2007, and at the International Conference on Acoustics, Speech and Signal Processing (ICASSP 2008), Las Vegas, USA, Apr. 2008.

power subject to predefined users' quality-of-service (QoS) targets, in a flat-fading environment. The transmitter will be provided with imperfect channel estimates and with the bounds on the uncertainty regions, which surely contain the exact channel values (contrary to [21], our focus is on erroneous channels and not on disturbed channel covariance matrices). In the cases where the receivers' equalizers should be designed, it is also supposed that the users either know their channels perfectly, or that there exists an error-free mechanism in the system, which delivers scaling coefficients to the users. This formulation presents one way of defining a robust counterpart of the standard downlink beamforming problem, whose solution in the perfect CSI case is known from [21]–[24]. The considered robust scenario is considerably more involved due to the fact that the QoS requirements must be supported for an infinite number of possible channels, contained in the uncertainty regions, with a single set of filters.

A. Related Work and Contributions

As QoS constraints, maximum allowable mean square errors (MSEs), or minimum tolerated signal-to-interference-plus-noise-ratios (SINRs) will be considered. The related robust problems in the single user, multiple-input multiple-output (MIMO) setting were analyzed in [16], [19], [25]. Two approaches emerged recently to cope with specific aspects that appear in a multiuser MISO setup: the MSE-constrained robust power control studied in [26], and robust precoding with SINR targets proposed in [27]. The main contributions of this paper can be briefly summarized as follows:

- We solve the MSE-constrained problem by optimizing the system *completely* using semidefinite programming (SDP) methods [28]. Thereby the performance of the solution from [26], that aimed at power control only and had the beamforming matrix fixed, is improved, with an acceptable increase in computational complexity.
- The SINR-constrained problem, posed originally in [27] with conservative solutions provided, is shown to have an optimal solution, based on the computationally involved ellipsoid method [29].
- By applying the derived MSE-optimization framework, an elegant conservative solution for the SINR-problem is found, which outperforms the related results from the literature in terms of performance-complexity tradeoff. This yielded a unifying framework for handling both types of QoS constraints.
- Besides the standard ellipsoidal uncertainty assumption, methods for supporting somewhat less-understood box-like error models, that completely change the mathematical structure of the problems, are derived, as well.

In this work, our focus was mainly on optimization techniques with the developed convergence theory. In other words, there exist upper bounds for the maximum number of iterations and arithmetical operations necessary for the termination of the algorithms, which should grow slowly with the size of the problem. We remark that after completing this paper, a parallel work on similar problems [30], [31] has been brought to our attention.

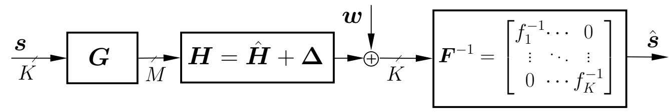

Fig. 1. Block-scheme of the studied multiuser MISO system.

B. Notation

Small and large bold fonts are used to denote vectors and matrices, respectively. If not explicitely stated, the dimensions will be clear from the context. $\boldsymbol{I}$ is the identity matrix and $\boldsymbol{0}$ is the zero-matrix. $\boldsymbol{A} \succeq \boldsymbol{B}$ means that $\boldsymbol{A} - \boldsymbol{B}$ is positive semidefinite ($\succ$ is used for the positive definiteness) [32]. The trace of a matrix is denoted with $\mathrm{Tr}\{\cdot\}$. $\|(\cdot)\|_1$, $\|(\cdot)\|_2$ and $\|(\cdot)\|_F$ denote the l_1-norm, the spectral norm and the Frobenius norm, respectively [33]. The matrix transpose, the conjugate (Hermitian) transpose and the Moore-Penrose pseudoinverse are written as $(\cdot)^T$, $(\cdot)^*$ and $(\cdot)^\dagger$, respectively. $\boldsymbol{A}_{(k,m)}$ is the element in the position (k,m) of $\boldsymbol{A}$, while $\boldsymbol{A}_{(:,m)}$ and $\boldsymbol{A}_{(k,:)}$ are the mth column and kth row of $\boldsymbol{A}$, respectively. The standard indexing with subscripts is used to denote an element of a vector. The vector $\mathrm{vec}(\boldsymbol{A})$ contains the columns of the matrix $\boldsymbol{A}$, stacked below each other. $\mathrm{diag}(a_1, \ldots, a_K)$ is a diagonal $K \times K$ matrix having elements $a_1, \ldots, a_K$ on the main diagonal. $\Re\{\cdot\}$ and $\Im\{\cdot\}$ extract real and imaginary parts of the argument, respectively. $\mathrm{E}\{\cdot\}$ is the expectation operator.

C. Outline of the Paper

The rest of the paper is organized as follows. In Section II, the system model is introduced. Section III formulates the MSE-constrained problem statement and provides an SDP-based solution. Robust precoders for a system with SINR targets are derived in Section IV. The rectangular uncertainty sets are analyzed in Section V. Simulation results are shown in Section VI, and the paper is concluded with a short summary in Section VII.

II. System Model

Consider a multiuser MISO system with K single-antenna users, where the BS is equipped with M antennas, as illustrated in Fig. 1. In one time instant, the BS transmits K independent symbols $s_1, s_2, \ldots, s_K$, where the symbol s_k is intended for the kth user.[1] To simplify the expressions, we group the transmit symbols into a vector $\boldsymbol{s}$, $\boldsymbol{s} = \begin{bmatrix} s_1 & s_2 & \ldots & s_K \end{bmatrix}^T$, with $\mathrm{E}(\boldsymbol{s}\boldsymbol{s}^*) = \boldsymbol{I}$ assumed, w.l.o.g.

The complete downlink, flat-fading channel is represented with the matrix $\boldsymbol{H}$, $\boldsymbol{H} \in \mathbb{C}^{K \times M}$. If multicarrier techniques, like orthogonal frequency division multiplexing (OFDM) [35], are employed to combat the intersymbol interference in frequency selective channels, the used model in this paper would correspond to the performance analysis for one subcarrier (see also [19], [36] for other ways of providing robustness in multi-antenna systems with frequency-selective channels).

[1]We note that the problems of broadcasting and multicasting, where common information is transmitted to certain groups of users, are significantly different [34].

The channel of the kth user is given as $\boldsymbol{H}_{(k,:)}$. It is assumed that the BS knows only erroneous channel estimates $\hat{\boldsymbol{H}}_{(k,:)}$, with

$$\boldsymbol{H}_{(k,:)} = \hat{\boldsymbol{H}}_{(k,:)} + \boldsymbol{\Delta}_{(k,:)}, \quad \forall k \in \{1, \ldots, K\}, \tag{1}$$

where $\boldsymbol{\Delta}_{(k,:)}$ is the error in the channel knowledge. The BS is also supposed to know the structure of the uncertainty regions $\mathcal{D}_k$, which surely contain the disturbances $\boldsymbol{\Delta}_{(k,:)}$. The requirement on the CSI at the receivers will be commented in more detail in the following sections, depending on the problem of interest.

The transmit filter (precoder) of the BS is denoted by $\boldsymbol{G}$, $\boldsymbol{G} \in \mathbb{C}^{M\times K}$. The eventual equalization of the non-cooperating users, is represented with a diagonal matrix $\boldsymbol{F}$, $\boldsymbol{F} = \mathrm{diag}(f_1, f_2, \ldots, f_K)$, $f_k \in \mathbb{C}\setminus\{0\}$, and the inverses are used for convenience. Finally, the system equations for the K users can be written as

$$\hat{s}_k = \frac{1}{f_k}\left(\boldsymbol{H}_{(k,:)}\boldsymbol{G}\boldsymbol{s} + w_k\right), \quad \forall k \in \{1, \ldots, K\}, \tag{2}$$

where w_k is the additive noise at the reception, with $\boldsymbol{w} = \begin{bmatrix} w_1 & w_2 & \ldots & w_K \end{bmatrix}^T$, and $\hat{s}_k$ is the estimate of s_k. We assume that the transmit signals and the receive noise are uncorrelated, and that $\mathrm{E}(\boldsymbol{w}\boldsymbol{w}^*) = \mathrm{diag}(\sigma_1^2, \ldots, \sigma_K^2)$ holds.

III. Robust MSE-Constrained Optimization

In this section, the MSEs will be adopted as the QoS measure, with

$$\mathrm{MSE}_k = \mathrm{E}\left\{|s_k - \hat{s}_k|^2\right\}, \quad \forall k \in \{1, \ldots, K\}. \tag{3}$$

The robust MSE-optimization problem assumes the minimization of the total transmit power P,

$$P = \mathrm{E}\left\{\mathrm{Tr}(\boldsymbol{G}\boldsymbol{s}\boldsymbol{s}^*\boldsymbol{G}^*)\right\} = \|\boldsymbol{G}\|_F^2, \tag{4}$$

subject to predefined MSE targets μ_k, which must be satisfied under uncertainty:

$$\min_{\boldsymbol{G}, f_1, \ldots, f_K} \quad P, \tag{5}$$

$$\text{s.t. } \mathrm{MSE}_k \le \mu_k, \quad \forall \boldsymbol{\Delta}_{(k,:)} \in \mathcal{D}_k,\ k = 1, \ldots, K. \tag{6}$$

The problem (5)-(6) is meant to be solved by the BS, having in mind that it possesses only imperfect CSI. As far as the users are concerned, in this section, it is assumed that there either exists an error-free control mechanism in the system that delivers the equalization coefficients from the BS to the users, or that the users have the perfect CSI, which is, comparing to the availability of the CSI at the transmit side, generally considered as less critical in practice. In the latter case, after the BS calculates its filter $\boldsymbol{G}$, the receivers would estimate the equivalent channels $\boldsymbol{H}^e_{(k,:)} = \boldsymbol{H}_{(k,:)}\boldsymbol{G}$ and adopt the standard minimum MSE (MMSE) solutions for their equalization coefficients f_k, with

$$f_k^{-1} = \left(\boldsymbol{H}^e_{(k,:)}{\boldsymbol{H}^e_{(k,:)}}^* + \sigma_k^2\right)^{-1}\boldsymbol{G}^*_{(:,k)}\boldsymbol{H}^*_{(k,:)}. \tag{7}$$

This approach will result in the obtained MSEs that surely also comply to the uncertain constraints (6), but without reducing the transmit power, obtained as the solution of (5)-(6). The key idea in optimizing the scaling factors in (5)-(6) is that the BS determines its beamformer $\boldsymbol{G}$ by having some (partial) knowledge of what could be done at the reception, which, as it will be shown in Section VI, yields significant gains. Finally, we note that the incorporation of the MMSE solution (7) immediately into the problem formulation (5)-(6) would yield problems of significantly more complex structure, as discussed in Section IV.

The problem (5)-(6), with the assumption of having the perfect CSI at both sides, can be solved using the methodology derived in [21]–[23]. We approach the uncertain problem (5)-(6) using numerical methods from convex optimization theory [32]. Firstly, we notice that the MSE expression of the kth user can be written as

$$\mathrm{MSE}_k = \frac{1}{|f_k|^2}\left((\boldsymbol{H}_{(k,:)}\boldsymbol{G} - f_k\boldsymbol{e}_k^*)(\boldsymbol{H}_{(k,:)}\boldsymbol{G} - f_k\boldsymbol{e}_k^*)^* + \sigma_k^2\right) \tag{8}$$

where $\boldsymbol{e}_k$ are standard basis vectors of $\mathbb{R}^K$ [33]. From (8), it can be concluded that assuming $f_k \in \mathbb{R}_{++}$ would not change the solution for the minimal transmit power of the optimization problem (5)-(6), due to the possibility of multiplying the columns of $\boldsymbol{G}$ with complex numbers of unit magnitude, without changing the objective function in (5). Therefore, we can proceed with the equivalent representation of the kth user's constraint

$$\mathrm{MSE}_k \le \mu_k \ \Leftrightarrow\ \left\|\begin{bmatrix} \boldsymbol{H}_{(k,:)}\boldsymbol{G} - f_k\boldsymbol{e}_k^* & \sigma_k \end{bmatrix}\right\|_2 \le f_k\sqrt{\mu_k}. \tag{9}$$

The convexity of the problem (5)-(6) can be proved now for any uncertainty region $\mathcal{D}_k$.

Theorem 1: The problem (5)-(6) is convex, irrespectively of the shape of the uncertainty regions $\mathcal{D}_k$.

Proof: Being the squared Frobenius norm of the transmit filter matrix $\boldsymbol{G}$, the objective function in (5) is clearly convex [32]. Consider now the kth user's constraint (9) under uncertainty. For any $\boldsymbol{H}_{(k,:)}$ from the uncertainty regions defined by $\hat{\boldsymbol{H}}_{(k,:)}$ and $\mathcal{D}_k$, (9) is a second-order cone constraint, which yields a convex feasible set for the unknown transceiver parameters [32]. The complete domain of (9) is the intersection of all such convex sets, corresponding to each channel from the uncertainty region $\hat{\boldsymbol{H}}_{(k,:)} + \boldsymbol{\Delta}_{(k,:)}$, $\boldsymbol{\Delta}_{(k,:)} \in \mathcal{D}_k$. Since the convexity is preserved under intersection [32], we conclude that the domain of (9) is also convex. Finally, the complete problem domain, defined by (6), is again convex as the intersection of the domains related to the constraints (9), with $k = 1, \ldots, K$. ■

Although the problem of interest is convex, it is still not clear if it can be efficiently solved, because of the uncertainty. In the sequel, we derive efficient numerical solutions for the often used, ball uncertainty model

$$\left\|\boldsymbol{\Delta}_{(k,:)}\right\|_2 \le \varepsilon_k, \quad \forall k \in \{1, \ldots, K\}. \tag{10}$$

The model (10) naturally captures well the bounded disturbances that are a result of quantization (see also Section VI), but it is convenient for representing the CSI errors with Gaussian distribution and optimizing the outage performance [18], [26], as well. In Section V, we analyze in more detail the case where the uncertainty regions are boxes.

Since the objective function in (5) is relatively simple, we focus in the sequel on the transformation of the uncertain constraints (6) into a tractable form. The following equivalent representation of (9), obtained as a direct application of the Schur Complements lemma [33] on (9), will be of great use in the further robust optimization

$$\boldsymbol{\Phi}_k + \begin{bmatrix} 0 & \boldsymbol{\Delta}_{(k,:)}\boldsymbol{G} & 0 \\ \boldsymbol{G}^*\boldsymbol{\Delta}^*_{(k,:)} & \mathbf{0} & \mathbf{0} \\ 0 & \mathbf{0} & 0 \end{bmatrix} \succeq \mathbf{0}, \ \forall \left\|\boldsymbol{\Delta}_{(k,:)}\right\|_2 \le \varepsilon_k, \quad \forall k \in \{1,\ldots,K\}, \tag{11}$$

where

$$\boldsymbol{\Phi}_k = \begin{bmatrix} f_k\sqrt{\mu_k} & \hat{\boldsymbol{H}}_{(k,:)}\boldsymbol{G} - f_k\boldsymbol{e}_k^* & \sigma_k \\ \boldsymbol{G}^*\hat{\boldsymbol{H}}^*_{(k,:)} - f_k\boldsymbol{e}_k & f_k\sqrt{\mu_k}\boldsymbol{I} & \mathbf{0} \\ \sigma_k & \mathbf{0} & f_k\sqrt{\mu_k} \end{bmatrix}. \tag{12}$$

To obtain a computationally tractable form from (11), we use the following lemma:

Lemma 1: Let $\boldsymbol{A}$, $\boldsymbol{B}$ and $\boldsymbol{C}$ be given matrices, with $\boldsymbol{A} = \boldsymbol{A}^*$. The relation

$$\boldsymbol{A} \succeq \boldsymbol{B}^*\boldsymbol{D}\boldsymbol{C} + \boldsymbol{C}^*\boldsymbol{D}^*\boldsymbol{B}, \quad \forall \boldsymbol{D} : \|\boldsymbol{D}\|_2 \le \varepsilon, \tag{13}$$

is valid, if and only if

$$\exists\lambda \ge 0, \quad \begin{bmatrix} \boldsymbol{A} - \lambda\boldsymbol{B}^*\boldsymbol{B} & -\varepsilon\boldsymbol{C}^* \\ -\varepsilon\boldsymbol{C} & \lambda\boldsymbol{I} \end{bmatrix} \succeq \mathbf{0}. \tag{14}$$

Proof: The proof, based on the $\mathcal{S}$-lemma [29], [32], [37], can be found in [16]. ∎

Now, we are equipped with the tools for rewriting the uncertain constraint (11) into a form that is convenient for the numerical analysis.

Theorem 2: The uncertain MSE constraints in (6), with the uncertainty regions $\mathcal{D}_k$ defined by (10), are equivalent to the linear matrix inequalities (LMIs) in the unknown transceiver coefficients

$$\begin{bmatrix} f_k\sqrt{\mu_k} - \lambda_k & \hat{\boldsymbol{H}}_{(k,:)}\boldsymbol{G} - f_k\boldsymbol{e}_k^* & \sigma_k & \mathbf{0} \\ \boldsymbol{G}^*\hat{\boldsymbol{H}}^*_{(k,:)} - f_k\boldsymbol{e}_k & f_k\sqrt{\mu_k}\boldsymbol{I} & \mathbf{0} & -\varepsilon_k\boldsymbol{G}^* \\ \sigma_k & \mathbf{0} & f_k\sqrt{\mu_k} & \mathbf{0} \\ \mathbf{0} & -\varepsilon_k\boldsymbol{G} & \mathbf{0} & \lambda_k\boldsymbol{I} \end{bmatrix} \succeq \mathbf{0}, \quad \forall k \in \{1,\ldots,K\}, \tag{15}$$

where λ_k are slack variables.

Proof: The LMIs in (15) are obtained by a direct application of Lemma 1 on the derived, equivalent representations (11) of the users' uncertain MSE constraints, with $\boldsymbol{A} = \boldsymbol{\Phi}_k$, $\boldsymbol{D} = \boldsymbol{\Delta}_{(k,:)}$, $\varepsilon = \varepsilon_k$ and

$$\boldsymbol{B} = -\begin{bmatrix} 1 & \mathbf{0} & \mathbf{0} \end{bmatrix}, \quad \boldsymbol{C} = \begin{bmatrix} \mathbf{0} & \boldsymbol{G} & \mathbf{0} \end{bmatrix}. \tag{16}$$

∎

It can be noticed that the objective function in (5) can be immediately resolved by introducing one slack variable t that should be minimized and a rotated second-order cone constraint $\|\mathrm{vec}(\boldsymbol{G})\|_2^2 \le t$. Therefore, under the uncertainty model (10), the problem (5)-(6) is equivalent to an SDP problem (more rigorously, this is a linear conic optimization problem with second order and semidefinite cones) and can be solved with interior point methods in a very efficient manner [28], [29], [38].

At this point, we notice that the practical per-antenna power constraints can be easily introduced into the derived semidefinite program, since they can be expressed as convex quadratic constraints

$$\left\|\boldsymbol{G}_{(m,:)}\right\|_2 \le \sqrt{P_m}, \quad m = 1,\ldots,M, \tag{17}$$

where P_m is the power limit for antenna m. This possibility of extension holds for all problems studied in this paper. Furthermore, the uncertainty at the transmitter with respect to the knowledge of the noise variances can also be incorporated in a straightforward manner. Finally, instead of balls, arbitrary ellipsoids of the form

$$\left\|\boldsymbol{V}\boldsymbol{\Delta}^T_{(k,:)}\right\|_2 \le 1, \tag{18}$$

with given $\boldsymbol{V} \succ \mathbf{0}$, can also be supported as uncertainty regions for the kth user's channel (notice that for $\boldsymbol{V} = \frac{1}{\varepsilon_k}\boldsymbol{I}_M$, the model (10) is obtained). A simple substitution $\boldsymbol{V}\boldsymbol{\Delta}^T_{(k,:)} = \underline{\boldsymbol{\delta}}_k$, $\|\underline{\boldsymbol{\delta}}_k\|_2 \le 1$ and the replacement of $\boldsymbol{\Delta}_{(k,:)}$ in the LMI (11) with $\underline{\boldsymbol{\delta}}_k^T\boldsymbol{V}^{-1}$, enable again the application of Lemma 1 and an SDP reformulation similar to that in Theorem 2. This is of particular importance, since there exist numerous methods for calculating the unique minimum volume ellipsoid that contains a certain set [29]. In that way, conservative tractable approximations can be obtained for a large class of uncertainty regions. We will return to this concept briefly also in Section VI.

IV. SINR as the Performance Measure

Consider the system model described in Section II. The SINR of the kth user can be calculated as

$$\mathrm{SINR}_k = \frac{|\boldsymbol{H}_{(k,:)}\boldsymbol{G}_{(:,k)}|^2}{\sum_{l=1,\, l\neq k}^{K}|\boldsymbol{H}_{(k,:)}\boldsymbol{G}_{(:,l)}|^2 + \sigma_k^2}. \tag{19}$$

Let the uncertainty model be defined as in (10). We can now formulate a robust counterpart of the standard SINR-constrained downlink beamforming problem

$$\begin{aligned} \min_{\boldsymbol{G}} \quad & P, \\ \text{s.t.} \quad & \mathrm{SINR}_k \ge \gamma_k, \quad \forall \left\|\boldsymbol{\Delta}_{(k,:)}\right\|_2 \le \varepsilon_k, \quad \forall k \in \{1,\ldots,K\}, \end{aligned} \tag{20}$$

where γ_k are the required QoS targets, expressed in terms of minimum tolerable SINRs.

The problem (20) is an involved, non-convex problem. This can be concluded by rewriting its constraints into a form

$$\begin{aligned} &\left\|\begin{bmatrix} \boldsymbol{H}_{(k,:)}\boldsymbol{G} & \sigma_k \end{bmatrix}\right\|_2 \le \sqrt{1+\gamma_k^{-1}}\,\left|\boldsymbol{H}_{(k,:)}\boldsymbol{G}_{(:,k)}\right|, \\ &\forall \left\|\boldsymbol{\Delta}_{(k,:)}\right\|_2 \le \varepsilon_k, \end{aligned} \tag{21}$$

which, due to the existence of the uncertainty on both sides and the absolute values, has, to the best of our knowledge, no tractable representation. Therefore, we formulate the following problem of interest

$$\begin{aligned} &\min_{\tilde{\boldsymbol{G}}} \quad \frac{1}{2}\left\|\tilde{\boldsymbol{G}}\right\|_F^2, \\ &\text{s.t.} \quad \left\|\left[\begin{array}{cc} \tilde{\boldsymbol{H}}_{(k,:)}\tilde{\boldsymbol{G}} & \sigma_k \end{array}\right]\right\|_2 \leq \sqrt{1+\gamma_k^{-1}}\,\tilde{\boldsymbol{H}}_{(k,:)}\tilde{\boldsymbol{G}}_{(:,k)}, \\ &\forall \left\|\tilde{\boldsymbol{\Delta}}_{(k,:)}\right\|_2 \leq \varepsilon_k, \quad \forall k \in \{1,\ldots,K\}, \end{aligned} \tag{22}$$

where

$$\tilde{\boldsymbol{H}}_{(k,:)} = \left[\begin{array}{cc} \Re\{\boldsymbol{H}_{(k,:)}\} & \Im\{\boldsymbol{H}_{(k,:)}\} \end{array}\right], \tag{23}$$

$$\tilde{\boldsymbol{\Delta}}_{(k,:)} = \left[\begin{array}{cc} \Re\{\boldsymbol{\Delta}_{(k,:)}\} & \Im\{\boldsymbol{\Delta}_{(k,:)}\} \end{array}\right], \tag{24}$$

$$\tilde{\boldsymbol{G}} = \left[\begin{array}{cc} \Re\{\boldsymbol{G}\} & \Im\{\boldsymbol{G}\} \\ -\Im\{\boldsymbol{G}\} & \Re\{\boldsymbol{G}\} \end{array}\right]. \tag{25}$$

In [21], [24], it is proved that the non-robust variations of (20) and (22) are equivalent. The idea was in showing that the term $\boldsymbol{H}_{(k,:)}\boldsymbol{G}_{(:,k)}$ in the numerator of (19) can be real and positive, w.l.o.g., which removes the absolute value in the right-hand side of (21), yields second-order cone constraints, and, consequently, a relatively simple conic quadratic optimization problem, whose real-valued version is exactly (22) with $\varepsilon_k = 0$. Unfortunately, the same principle is not applicable for the robust designs, due to the fact that an infinite number of channels must be supported with a single filter. However, the fulfillment of uncertain constraints in (22) clearly implies that the conditions (21) are also valid. Therefore, (22) can be viewed as a conservative approximation of (20). In other words, a filter obtained by solving (22) will surely be a feasible solution for (20), as well. However, the feasible set of (22) is smaller than in (20), so it is more likely to have infeasible scenarios, and the resulting transmit power from solving (22) is an upper bound for the optimal solution of (20). Finally, we note that in the SINR-constrained problem formulations, no particular requirement on the CSI knowledge at the receive side is necessary, as the users' equalization plays no role in (19).

The problem (22) was posed originally in [27], where three further restrictions of (22) are optimally solved using tractable SDP reformulations. Notice that due to the existence of the uncertainty on both sides in the constraints in (22), rewriting these constraints as LMIs would not yield a suitable structure needed for the application of Lemma 1, as observed also in [27], [39]. We show in the sequel that the problem (22) can actually be solved optimally, by applying the ellipsoid method from convex optimization theory. Due to the fact that the ellipsoid method exhibits high (though still polynomial [29]) complexity, we derive then an efficient SDP-based suboptimal solution for the same problem, which exhibits better properties in terms of both performance and complexity, w.r.t. the related results from the literature. Furthermore, a comparison by numerical simulations will reveal that this SDP-based conservative solution seems to perform as well as the theoretically optimal benchmark provided by the ellipsoid method.

A. Solution by the Ellipsoid Method

The ellipsoid method presents a multidimensional extension of the bisection approach. The main idea behind the algorithm can be formulated as follows. At a given iteration we are equipped with an ellipsoid which surely contains the optimal solution and check whether the center of the ellipsoid is in the problem domain. If that is the case, a subgradient of the objective function in the center of the ellipsoid should be calculated. Zero value of the subgradient means that the optimal solution is found, otherwise, the subgradient defines a hyperplane and, consequently, a half-ellipsoid, which contains the optimal solution. In the latter case, the new search ellipsoid is the minimal volume ellipsoidal container of the described half-ellipsoid. If the center of the ellipsoid is not in the problem domain, the hyperplane that separates the center from the problem domain can be constructed to obtain a new half-ellipsoid whose minimal volume ellipsoidal container is used for the subsequent search. The procedure yields a sequence of the shrinking ellipsoids which converges to the optimal solution.

We start with recalling the ellipsoid method in Algorithm 1, as described in [29], omitting the technical details regarding the initialization and the formalization of the convergence criterion. The unknown vector to be calculated, which uniquely determines the transmit filter $\boldsymbol{G}$, is denoted by

$$\boldsymbol{g} = \left[\begin{array}{ccc} \tilde{\boldsymbol{G}}_{(:,1)}^T & \cdots & \tilde{\boldsymbol{G}}_{(:,K)}^T \end{array}\right]^T \in \mathbb{R}^d, \tag{26}$$

where $d = 2MK$. Notice that in Algorithm 1, $\bar{\boldsymbol{g}}_t$ is the sequence of the search ellipsoids' centers, while in each iteration the vector $\boldsymbol{a}_t$ defines the hyperplane that divides the current search ellipsoid.

Algorithm 1 Algorithmic solution for the robust, SINR-constrained precoder.

Initialize the first search ellipsoid $\{\bar{\boldsymbol{g}}_0 + \boldsymbol{B}_0\boldsymbol{u}, \|\boldsymbol{u}\|_2 \leq 1\}$. Set $t = 0$ (step number).
repeat
  $t \leftarrow t + 1$.
  if $\bar{\boldsymbol{g}}_{t-1} \in \mathcal{S}$, where $\mathcal{S}$ is the domain of (22): Calculate the vector $\boldsymbol{a}_t$ as the subgradient of the objective function in $\bar{\boldsymbol{g}}_{t-1}$. If $\boldsymbol{a}_t = \boldsymbol{0}$ the optimal solution is $\bar{\boldsymbol{g}}_{t-1}$. Skip the following step.
  if $\bar{\boldsymbol{g}}_{t-1} \notin \mathcal{S}$: Calculate the separation vector $\boldsymbol{a}_t$ that satisfies

$$\boldsymbol{a}_t^T\bar{\boldsymbol{g}}_{t-1} \geq \sup_{\boldsymbol{g}\in\mathcal{S}} \boldsymbol{a}_t^T\boldsymbol{g}, \quad \boldsymbol{a}_t \neq \boldsymbol{0}. \tag{27}$$

  Update the search ellipsoid:

$$\boldsymbol{p}_t = \frac{\boldsymbol{B}_{t-1}^T\boldsymbol{a}_t}{\sqrt{\boldsymbol{a}_t^T\boldsymbol{B}_{t-1}\boldsymbol{B}_{t-1}^T\boldsymbol{a}_t}}, \; \bar{\boldsymbol{g}}_t = \bar{\boldsymbol{g}}_{t-1} - \frac{1}{d+1}\boldsymbol{B}_{t-1}\boldsymbol{p}_t \tag{28}$$

$$\boldsymbol{B}_t = \frac{d\boldsymbol{B}_{t-1}}{\sqrt{d^2-1}} + \left(\frac{d}{d+1} - \frac{d}{\sqrt{d^2-1}}\right)\boldsymbol{B}_{t-1}\boldsymbol{p}_t\boldsymbol{p}_t^T \tag{29}$$

until : convergence is reached

We formulate the main conclusion of this section as a theorem:

Theorem 3: The sequence $\bar{\boldsymbol{g}}_t$ from Algorithm 1 converges to the optimal solution of the problem (22). The feasibility check for $\bar{\boldsymbol{g}}_{t-1}$ and the construction of $\boldsymbol{a}_t$ can be efficiently performed, and the complexity of Algorithm 1 is polynomial.

Proof: The proof is given in Appendix A. ∎

B. SDP-Based Solution

In this section, we approach the problem (22) indirectly. Define a virtual MSE-optimization problem (5)-(6), with the same channels and with QoS targets

$$\mu_k = \frac{1}{1+\gamma_k}, \quad \forall k \in \{1, \ldots, K\}. \tag{30}$$

It is known that if perfect CSI is provided at both sides, such MSE-constrained problem is equivalent to (22) and (20), as far as the transmit filter is concerned [23]. The following theorem shows that in the robust case, the virtual MSE-optimization problem can serve as a conservative, tractable approximation of (22) and consequently (20).

Theorem 4: Let the MSE problem (5)-(6) be feasible with the targets $\mu_k \in (0,1)$, $k = 1, \ldots, K$, and let $\boldsymbol{G}_{\text{opt}}$ be the resulting optimal transmit filter. The SINR constraints in (22) are satisfied then for γ_k obtained from (30), with the same transmit filter $\boldsymbol{G}_{\text{opt}}$.

Proof: It can be seen that the condition $\text{MSE}_k \leq \mu_k$ is equivalent to

$$\sum_{l=1,\, l\neq k}^{K} \left| \frac{1}{f_k} \boldsymbol{H}_{(k,:)} \boldsymbol{G}_{(:,l)} \right|^2 + \left| \frac{1}{f_k} \boldsymbol{H}_{(k,:)} \boldsymbol{G}_{(:,k)} - 1 \right|^2 + \frac{\sigma_k^2}{f_k^2} \leq \mu_k. \tag{31}$$

Since $f_k > 0$ and $\mu_k \in (0,1)$, it follows that $\Re\{\boldsymbol{H}_{(k,:)}\boldsymbol{G}_{(:,k)}\} \geq 0$, because otherwise the absolute value of $\Re\left\{\frac{1}{f_k}\boldsymbol{H}_{(k,:)}\boldsymbol{G}_{(:,k)} - 1\right\}$ would be larger than 1. Therefore, it is sufficient to prove that $\text{MSE}_k \leq \mu_k$ implies

$$\left\| \begin{bmatrix} \boldsymbol{H}_{(k,:)}\boldsymbol{G} & \sigma_k \end{bmatrix} \right\|_2^2 \leq \frac{1}{1-\mu_k} \left(\Re\{\boldsymbol{H}_{(k,:)}\boldsymbol{G}_{(:,k)}\} \right)^2, \tag{32}$$

since $1+\gamma_k^{-1} = (1-\mu_k)^{-1}$, $\Re\left\{\boldsymbol{H}_{(k,:)}\boldsymbol{G}_{(:,k)}\right\} = \tilde{\boldsymbol{H}}_{(k,:)}\tilde{\boldsymbol{G}}_{(:,k)}$, and the spectral norms of vectors $\begin{bmatrix} \boldsymbol{H}_{(k,:)}\boldsymbol{G} & \sigma_k \end{bmatrix}$ and $\begin{bmatrix} \tilde{\boldsymbol{H}}_{(k,:)}\tilde{\boldsymbol{G}} & \sigma_k \end{bmatrix}$ are equal, so the SINR constraints in (22) would be fulfilled. We proceed by rewriting (31) into an equivalent form

$$\begin{aligned} \left\| \begin{bmatrix} \boldsymbol{H}_{(k,:)}\boldsymbol{G} & \sigma_k \end{bmatrix} \right\|_2^2 \leq f_k^2\mu_k + \left|\boldsymbol{H}_{(k,:)}\boldsymbol{G}_{(:,k)}\right|^2 \\ - \left|\boldsymbol{H}_{(k,:)}\boldsymbol{G}_{(:,k)} - f_k\right|^2. \end{aligned} \tag{33}$$

The theorem is proved by noticing that

$$\begin{aligned} f_k^2\mu_k + \left|\boldsymbol{H}_{(k,:)}\boldsymbol{G}_{(:,k)}\right|^2 - \left|\boldsymbol{H}_{(k,:)}\boldsymbol{G}_{(:,k)} - f_k\right|^2 \\ \leq \frac{1}{1-\mu_k}\left(\Re\{\boldsymbol{H}_{(k,:)}\boldsymbol{G}_{(:,k)}\}\right)^2 \end{aligned} \tag{34}$$

is true, because it is equivalent to

$$\left(\Re\{\boldsymbol{H}_{(k,:)}\boldsymbol{G}_{(:,k)}\} - f_k(1-\mu_k)\right)^2 \geq 0. \tag{35}$$

∎

The problem (22) can now be approached in the following way: For a fixed set of targets $\text{SINR}_k \geq \gamma_k$, the virtual MSE constraints $\text{MSE} \leq \mu_k$ are defined using (30). The problem (5)-(6) is solved then by applying the SDP method from Section III, and the resulting transmit filter surely complies to the specified SINR requirements γ_k. The excellent quality of this approximation with respect to the optimal solution from Section IV-A will be seen from simulation results in Section VI.

While we have shown how the optimal solution of (22) can be computed by employing the ellipsoid method, the optimal solution of the SINR-constrained problem (20) remains as an open topic for the future work (see also the discussion after the definition of (22)). We remark also that if the perfect CSI is assumed at the reception side, and if the equivalent channels can be estimated, it can be easily proved that the application of the standard MMSE solution (7) for the receiver's coefficients in the MSE-constrained problem (5)-(6) would lead to the same non-convex problem (20). There lies the possibility for improving the performance for both QoS measures. However, due to the non-convexity of the problems, the price that has to be paid will probably be the increased or non-guaranteed computational complexity [40].

V. Rectangular Uncertainty Regions

In practical systems, the uncertainty regions in the form of boxes (hyperrectangles) might be of particular interest, with

$$\left|\Re\{\boldsymbol{\Delta}_{(k,m)}\}\right| \leq \varepsilon_k, \quad \left|\Im\{\boldsymbol{\Delta}_{(k,m)}\}\right| \leq \varepsilon_k, \tag{36}$$

for all $k = 1, \ldots, K$, $m = 1, \ldots, M$. Notice that we do not suggest any specific quantization scheme (scalar or vector), but just focus on another possible bounded error model. For convenience, we return to the MSE-optimization problem from Section III (having in mind also the ability to support the SINR-constrained problems, as explained in Section IV-B) and proceed by transforming the LMI in (11) into a tractable form, with respect to the model (36).

Theorem 5: The constraints in (6), with uncertainty regions specified by (36), are equivalent to the following set of LMIs

$$\boldsymbol{\Phi}_k + \sum_{m=1}^{M} v_m^{k,p}\boldsymbol{Y}_m + \sum_{m=1}^{M} v_{m+M}^{k,p}\boldsymbol{Z}_m \succeq \boldsymbol{0} \tag{37}$$

for all $k \in \{1, \ldots, K\}$ and all vectors $\boldsymbol{v}^{k,p}$, $p = 1, \ldots, 2^{2M}$, given as

$$\begin{aligned} \boldsymbol{v}^{k,p} &= \varepsilon_k \begin{bmatrix} v_1 & v_2 & \cdots & v_{2M} \end{bmatrix}^T, \\ v_1 = \pm 1, \ldots, v_{2M} = \pm 1, &\quad p = 1 + \sum_{l=1}^{2M} 2^{2M-l}\max\{v_l, 0\}, \end{aligned} \tag{38}$$

and where the matrices $\boldsymbol{Y}_m$ and $\boldsymbol{Z}_m$ are defined as

$$\boldsymbol{Y}_m = \begin{bmatrix} 0 & \boldsymbol{G}_{(m,:)} & 0 \\ \boldsymbol{G}_{(m,:)}^* & \boldsymbol{0} & \boldsymbol{0} \\ 0 & \boldsymbol{0} & 0 \end{bmatrix}, \tag{39}$$

$$\boldsymbol{Z}_m = \begin{bmatrix} 0 & j\boldsymbol{G}_{(m,:)} & 0 \\ -j\boldsymbol{G}_{(m,:)}^* & \boldsymbol{0} & \boldsymbol{0} \\ 0 & \boldsymbol{0} & 0 \end{bmatrix}. \tag{40}$$

Proof: Define for notational convenience vectors $\boldsymbol{\delta}^k$

$$\boldsymbol{\delta}^k = \left[\begin{array}{ccc} \delta_1^k & \dots & \delta_{2M}^k \end{array}\right]^T = \tilde{\boldsymbol{\Delta}}_{(k,:)}^T, \quad \forall k \in \{1,\dots,K\}. \tag{41}$$

with $\tilde{\boldsymbol{\Delta}}_{(k,:)}$ given by (24). The constraints (11) (and equivalently (6)) in the case of rectangular uncertainty regions (36) can be rewritten into a form

$$\boldsymbol{\Phi}_k + \sum_{m=1}^{M} \delta_m^k \boldsymbol{Y}_m + \sum_{m=1}^{M} \delta_{m+M}^k \boldsymbol{Z}_m \succeq \mathbf{0},$$
$$\forall \delta_l^k \in \mathbb{R} : |\delta_l^k| \leq \varepsilon_k, \quad l = 1,\dots,2M, \ \forall k \in \{1,\dots,K\}. \tag{42}$$

Consider (42) as an LMI in $\boldsymbol{\delta}^k$. The set of all error vectors $\boldsymbol{\delta}^k$ that represent one user's channel uncertainty is the convex hull of the finite set of fixed vectors $\boldsymbol{v}^{k,p}$, $p = 1,\dots,2^{2M}$. Therefore, due to the convexity of the LMIs (42) with respect to $\boldsymbol{\delta}^k$, the fulfillment of (37) is the necessary and sufficient condition for (42) to be valid, which concludes the proof. ∎

Similarly to Section III, the desired optimization can be performed in principle using the SDP methods. However, notice that the number of additional constraints (LMIs) corresponding to one user k, reflected in the index p, grows exponentially with the number of transmit antennas. Such behavior might prevent this approach from practical application, especially if the BS employs an antenna array with many elements. Therefore, having simpler, conservative (in the sense that the MSE targets are never violated) tractable approximations might be of significant interest in practice. The following theorem proposes one such approximation of the problem with lower computational burden.

Theorem 6: In the case of rectangular uncertainty regions (36), the constraints (6) are implied by the LMIs

$$\boldsymbol{\Upsilon}_m^k \succeq \pm \boldsymbol{Y}_m, \quad \boldsymbol{\Psi}_m^k \succeq \pm \boldsymbol{Z}_m, \quad m = 1,\dots,M, \tag{43}$$

$$\boldsymbol{\Phi}_k - \varepsilon_k \sum_{m=1}^{M} (\boldsymbol{\Upsilon}_m^k + \boldsymbol{\Psi}_m^k) \succeq \mathbf{0}, \ \forall k \in \{1,\dots,K\}, \tag{44}$$

where $\boldsymbol{\Upsilon}_m^k$ and $\boldsymbol{\Psi}_m^k$ are slack matrix variables, and $\boldsymbol{Y}_m$ and $\boldsymbol{Z}_m$ are defined by (39)-(40).

Proof: Notice that for arbitrary $\boldsymbol{\Upsilon}$, $\boldsymbol{Y}$ and $\varepsilon \geq 0$ the following relations are valid

$$\boldsymbol{\Upsilon} \succeq \pm \boldsymbol{Y} \quad \Leftrightarrow \quad \pm\varepsilon \boldsymbol{Y} \succeq -\varepsilon \boldsymbol{\Upsilon} \tag{45}$$

$$\Leftrightarrow \quad \delta \boldsymbol{Y} \succeq -\varepsilon \boldsymbol{\Upsilon}, \quad \forall \delta \in \mathbb{R} : |\delta| \leq \varepsilon, \tag{46}$$

where the equivalence relation (45) is obtained by a simple multiplication with $-\varepsilon$, and (46) follows from the same arguments based on the convex hull as in the proof of Theorem 5. Therefore, with the assumption (43), we conclude

$$\boldsymbol{\Phi}_k + \sum_{m=1}^{M} \delta_m^k \boldsymbol{Y}_m + \sum_{m=1}^{M} \delta_{m+M}^k \boldsymbol{Z}_m \succeq \boldsymbol{\Phi}_k - \varepsilon_k \sum_{m=1}^{M} (\boldsymbol{\Upsilon}_m^k + \boldsymbol{\Psi}_m^k), \tag{47}$$

for all $\boldsymbol{\delta}^k$ (41) that comply to (36), which completes the proof of the theorem. ∎

Contrary to the exact solution, the number of additional constraints for the procedure described by Theorem 6 increases only linearly with the number of transmit antennas M, which is clearly beneficial in terms of the decreased computational complexity, despite the additionally introduced slack variables. We discuss the quality of this approximation in more detail in Section VI.

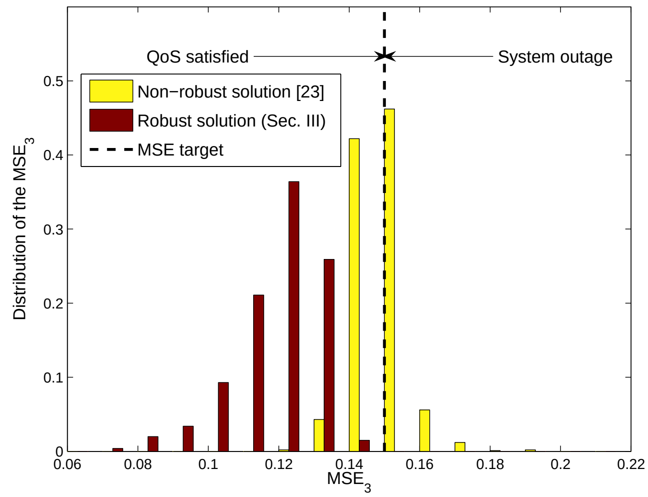

Fig. 2. Comparison of the robust (Section III) and non-robust [23] solutions in an MSE-constrained multiuser MISO system.

VI. Numerical Examples and Discussion

Except for the ellipsoid method from Section IV-A which is implemented directly, numerical simulations in this section are obtained obtained using SeDuMi [41].

We start with a simulation result that compares the robust and the non-robust solution of the MSE-optimization problem (5)-(6) in a 3-user system. The noise variance, the MSE targets and the bounds on the uncertainty (10) are assumed to be the same for all users: $\sigma_k^2 = 0.1$, $\mu_k = 0.15$ and $\varepsilon_k = 0.1$. The BS is equipped with $M = 4$ antennas. The distributions of the third user's MSE, if the non-robust solution from [23] and the robust solution from Section III are implemented, are plotted in Fig. 2 for 10^3 randomly chosen channel realizations which yielded feasible problems for the specified targets. The real and imaginary parts of each channel coefficient had normal distribution with zero mean and variance 0.5, and the errors were uniformly chosen from the uncertainty regions (10). It can be concluded that if the transceiver optimization is performed disregarding the disturbances, the system does not satisfy the QoS constraint for more than 50% of the channel realizations. Contrary to this, the robust algorithm proposed in Section III guarantees the targets all the time, and the system never experiences an outage.

For introducing robustness in the system, clearly, a certain price had to be paid. In the problem formulation (5)-(6), this would correspond to the increased transmit power with respect to the situation when the obtained channel knowledge was perfect. In Fig. 3, we compare the performance of the solution for the MSE-optimization problem from Section III with three strategies. The first one is the robust power allocation proposed in [26]. We plot also the result of optimization from Section III if the receivers are fixed, with $f_k = 1$, $k \in \{1, 2, 3\}$. Finally, the performance of the hypothetical system, where

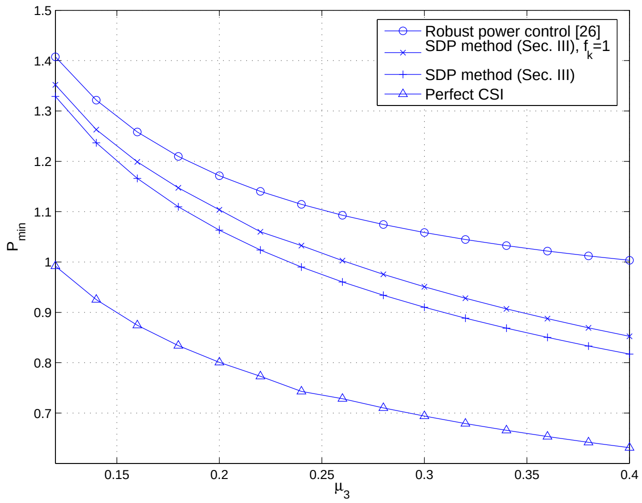

Fig. 3. Minimal transmit power versus the QoS (MSE) target of the third user, $\sigma^2_{1,2,3} = 0.1$, $\mu_{1,2} = 0.15$.

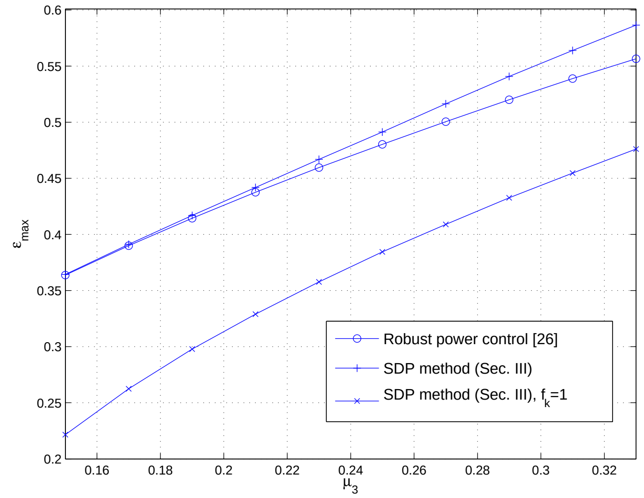

Fig. 4. Maximum size of the uncertainty set ε_k, assumed to be the same for all users, for the MSE-constrained problem.

σ_k^2	Per. CSI	SDP (Sec. III)	Pow. Con. [26]	SDP, $f_k = 1$
0.01	0.0011	0.0083	0.0112	0.0202
0.1	0.0056	0.0169	0.0208	0.1213

TABLE I
MINIMUM FEASIBLE MSE TARGET μ_3 IN A 3-USER MISO SYSTEM WITH $\mu_{1,2} = 0.15$.

the obtained CSI is correct, is given, as well. The minimum transmit power is plotted for various MSE targets μ_3 of the third user, with other simulation parameters being the same as in the previous example. The results present an average over 10^3 channels, chosen so that the problem was feasible for the observed range of QoS constraints. It can be seen that the proposed SDP-based solution from Section III outperforms in performance other robust strategies. The SDP-based robustness, which enabled the fulfillment of the targets, required roughly 25-35$\%$ more power comparing to the case when the obtained channel knowledge was exact. We remark that the performance gaps between the investigated strategies vary depending on the system size, the uncertainty level and the signal-to-noise ratio (noise power) in the system.

Due to the fact that the uncertain MSE constraints are shown to be LMIs, the feasibility range of the MSE constraints μ_k can be calculated by the bisection method [32]. In Table I, we list the average feasibility ranges of the MSE target of the third user μ_3, with $\mu_{1,2} = 0.15$ fixed, for two noise variances. Other system parameters are the same as in the first simulation example. Additionally, we imposed a total power constraint $P \leq 10$, which is introduced into the optimization framework in a straightforward manner, as discussed in Section III.

Similarly to the previous example, it can be concluded that the maximum size of the uncertainty ε_k is also readily obtained by the bisection method. This parameter is of importance in determining the roughness of the quantization that can be allowed in the CSI, e.g., when returning it from the receivers to the BS using the feedback channels. The averaged results with the same system parameters as for the example in Fig. 3, with the additional power constraint $P \leq 10$, and with the bounds ε_k assumed to be the same for all users, are given in Fig. 4. The results from Table I and Fig. 4 confirm that the proposed SDP-based approach exhibits better properties comparing to the other two robust methods also in terms of the feasibility regions and the sustained level of uncertainty.

In Fig. 5, we plot the Monte Carlo simulations for the minimum transmit power against the SINR targets, which are now assumed to be the same for all users. The system parameters are $M = K = 3$, $\sigma^2_{1,2,3} = 0.1$ and $\varepsilon_{1,2,3} = 0.1$. The results present an average over 2000 channel realizations that yielded feasible problems for the considered range of SINR targets. It can be seen that the solution based on the ellipsoid method and the SDP-based approach from Section IV perform the same. They both outperform the structured RSDP approach from [27]. Furthermore, the complexity of the proposed SDP-based method appears to be smaller comparing to the solution from [27], which employs larger LMIs and more unknown variables. The average number of iterations necessary for the termination of the algorithms in our implementation (the accuracy was 10^{-6} [41]) varied from 9.47 to 11.02 depending on the SINR target for our SDP solution, comparing to the 22.83 to 24.37 for the same parameters in the structured RSDP approach. The number of iterations for the ellipsoid method was typically of the order of 10^2. We remark that we performed no additional optimization of the code, and that the tailored application of the interior point algorithms, which could exploit further the structure of the problems, is beyond the scope of this paper. In Section VI-A, however, we present a brief theoretical analysis of the complexity of all investigated methods.

We finish the analysis of the SINR-constrained problem by plotting in Fig. 6 the percentage of feasible channel realizations in a system with the same parameters as in the previous simulation and the default SeDuMi settings used. The SINR target of 10 dB is assumed to be the same for all three users. 2000 randomly generated multiuser channels, with the complex Gaussian distribution of the channel coefficients remaining the same as for the first simulation result

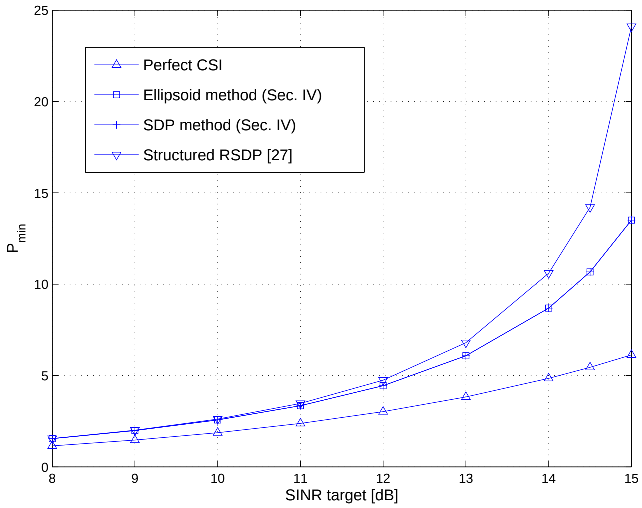

Fig. 5. Minimal transmit power versus the SINR target (assumed to be the same for all users) for a system with $\sigma^2_{1,2,3} = 0.1$ and $\varepsilon_{1,2,3} = 0.1$.

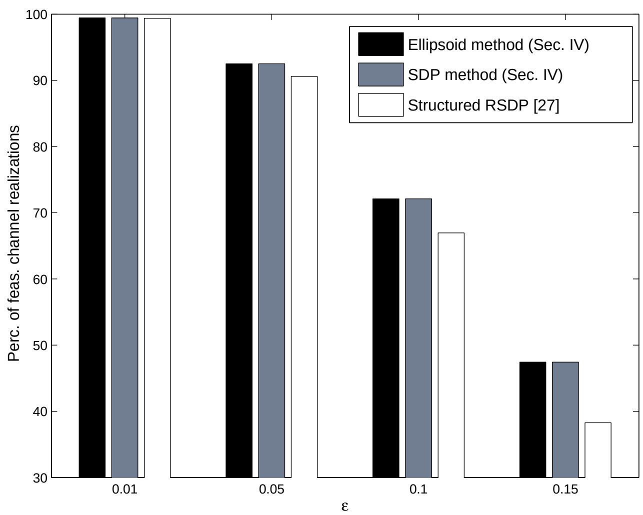

Fig. 6. Percentage of feasible channel realizations in a system with $M = K = 3$, $\sigma^2_{1,2,3} = 0.1$, $\varepsilon_{1,2,3} = 0.1$ and $\gamma_{1,2,3} = 10\,\text{dB}$.

in this section, were inspected. The conclusions regarding the performance ordering are similar as in the power minimization case.

Finally, in Fig. 7, we illustrate the algorithms for dealing with the rectangular quantization, described in Section V. The system parameters were $M = K = 3$, $\sigma^2_{1,2,3} = 0.1$, $\varepsilon_{1,2,3} = 0.01$ in (36) and $\mu_{1,2} = 0.1$. Minimum transmit power, averaged over 10^3 feasible random channel realizations, is plotted versus the MSE target of the third user μ_3. The exact and the approximate solution from Section V, the performance if the CSI is perfect, and a conservative approach, where the rectangular uncertainty regions are approximated by minimum volume balls containing them with the solution from Section III applied (the radius of these balls can be simply calculated as $\varepsilon_k\sqrt{2K}$), are compared. It can be seen that the approximate approach, derived in Section V, matches well for the most of the observed QoS range with the computationally involved exact method, while the computationally simplest spherical

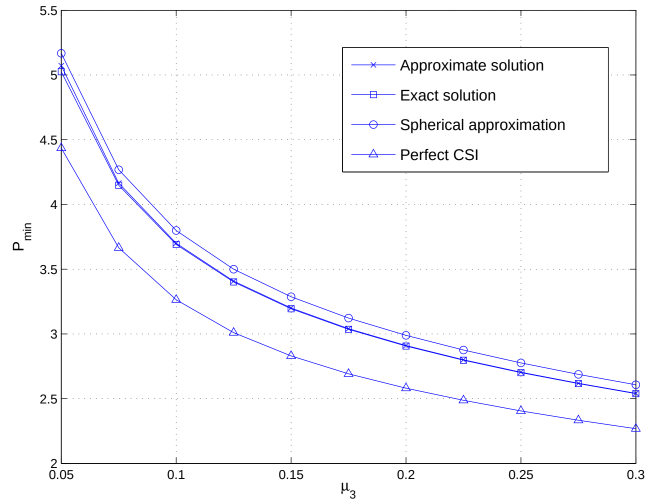

Fig. 7. Minimal transmit power for the rectangular quantization in a 3-user MISO system with $\mu_{1,2} = 0.1$.

approximation has somewhat worse performance if the target is far from the border of the feasibility region.

A. Notes on Computational Complexity

Except for the ellipsoid method from Section IV-A, that exhibits significantly larger computational burden [29], all studied methods in this paper and in the relevant results from the literature applied the SDP techniques, or they can be easily transformed into them for the sake of a rough comparison. The arithmetic complexity of the SDP programming methods depends significantly on the problem structure, and the detailed analysis is beyond the scope of this paper. However, a good insight can be gained already from studying the general bounds. Consider a standard real-valued semidefinite program $\min_{\boldsymbol{x}\in\mathbb{R}^n}\{\boldsymbol{c}^T\boldsymbol{x} :\ \boldsymbol{A}_0 + \sum_{i=1}^{i=n} x_i\boldsymbol{A}_i \succeq \boldsymbol{0},\ \|\boldsymbol{x}\|_2^2 \le R\}$, where $\boldsymbol{A}_i$ are symmetric block-diagonal matrices with m diagonal blocks of size $k_l \times k_l$, $l = 1, \ldots, m$. Stack all data that uniquely describe the system into a vector $\boldsymbol{d}$, and let s be the size of this vector. The number of elementary arithmetic operations necessary for determining the ϵ-solution is known to be upper-bounded by [29]

$$C = O(1)\left(1 + \sum_{l=1}^{m} k_l\right)^{1/2} n\left(n^2 + n\sum_{l=1}^{m} k_l^2 + \sum_{l=1}^{m} k_l^3\right) \times \ln\left(\frac{s + \|\boldsymbol{d}\|_1 + \epsilon^2}{\epsilon}\right). \tag{48}$$

Therefore, the key influence on the computational complexity is made by the size of the vector containing unknown variables n, and by the sizes of the LMIs k_l. We use these parameters to compare the examined strategies in this paper. The standard transformation of the objective function into a minimization of a linear function with slack variables and an LMI constraint, will be neglected, since this has a minor influence on the performance.

The SDP algorithm derived in Section III has $2MK + K$ original unknown values (real and imaginary parts of the transceiver coefficients) and K additional slack variables λ_k. There are K LMIs corresponding to the users' constraints with sizes $2(K+M+2)$ in the real-valued SDP representation. This also determines the complexity of the conservative SINR-optimization from Section IV-B, with the users' equalization coefficients treated as slack variables.

The solution from [26] is simpler firstly in the sense that only power allocation, i.e., only K real-valued coefficients $q_1, \ldots, q_K$ are optimized. These coefficients are tightly connected with the equalization scaling factors $f_1, \ldots, f_K$ from Fig. 1. The constraints in [26] are originally given in the form

$$\lambda_{\max}\left(\hat{\boldsymbol{H}}^{\dagger}\operatorname{diag}(q_1, \ldots, q_K)\hat{\boldsymbol{H}}^{\dagger^*}\right) \leq c_1 q_k + c_2, \tag{49}$$

where c_1 and c_2 are constants depending on the MSE targets, the noise variances and the sizes of the uncertainty regions, and $\lambda_{\max}(\cdot)$ denotes the maximum eigenvalue of a matrix. The condition (49) can be rewritten in the real-valued form $q_k \boldsymbol{I}_{2M} - \boldsymbol{X}(q_1, \ldots, q_K) \succeq \boldsymbol{0}$, where $\boldsymbol{X}$ depends affinely on the powers $q_1, \ldots, q_K$ [29].[2] Therefore, the size of the LMIs is $2M$ which is smaller comparing to the proposed solution in Section III. However, as seen from Fig. 3, Fig. 4 and Table I, the gains introduced by the proposed full optimization can be significant.

As far as the SINR-constrained downlink transmission is concerned, in [27], the size of the LMI and the number of additional slack variables corresponding to the kth user constraint are $2(K+1)(2M+1)$ and $(K+1)(2K+3)$, respectively, which is larger comparing to the same parameters in the solution based on the virtual MSE-optimization problem, that is also seen to exhibit better performances.

Finally, in the rectangular quantization case, studied in Section V, a qualitatively clear difference in complexity among the exact solution, which cannot be considered as solvable in polynomial time, and the approximate methods can be noticed. In a practical application, for the QoS targets close to the edges of the feasibility region, the spherical approximation would be preferred, while for the rest of the feasible region, the approximate solution, based on Theorem 6, could be of more interest.

VII. Conclusion

The unified framework for a robust support of minimum allowable SINR targets and maximum tolerable MSE constraints in a multiuser MISO setting has been derived. The algorithms are based on SDP methods and efficiently handle ellipsoidal uncertainty sets. The formulated MSE-optimization problem has been solved optimally, while a conservative tractable approximation, with performance that closely matches the derived, computationally more involved optimal solution, is provided for the SINR-constrained optimization. In both cases, however, the obtained methods are found to outperform in performance the related results from the literature. With the MSE as the QoS measure, a relatively small increase in complexity is observed, while in the SINR case the method appears to be even simpler than the known approaches. The convergence polynomial in time is guaranteed. In the case of rectangular uncertainty regions, besides an involved exact solution, conservative approximations with significantly smaller computational burden have been derived, with a minor loss in performance.

We remark also that the first results show promising possibilities for an application of the proposed framework in a more general multiuser context, where the receivers also have multiple antennas (multiuser MIMO systems), and for handling a broader range of optimization problems, such as the sum-MSE (SINR) optimization, fairness, etc. [42].

[2]We remark that in special cases of the problems studied in [26], there are possibilities for employing more efficient iterative algorithms than SDP.

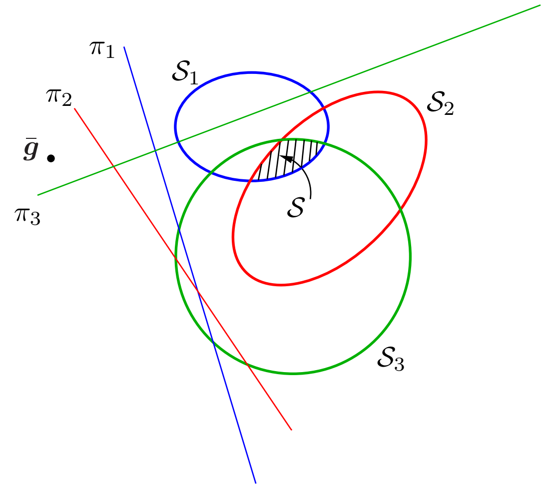

Fig. 8. Separation hyperplanes π_k, defined by (27), and the domains $\mathcal{S}_k$, that correspond to users' constraints in (22).

Appendix A
Proof of Theorem 3

In the sequel, it will be shown that all ingredients for Algorithm 1 are indeed available. The ability to construct the subgradient of the objective function is not problematic. Clearly, $P = \|\boldsymbol{g}\|_2^2$ is valid, and this function is differentiable, so its subgradient is equal to the usual gradient: $\partial P = 2\boldsymbol{g}$.

The problems of determining whether a particular vector $\boldsymbol{g} = \bar{\boldsymbol{g}}$ is feasible for (22) and the construction of the separation oracle, defined by (27), are considerably more involved. Notice that the domain $\mathcal{S}$ of (22) is an intersection of sets $\mathcal{S}_k$, $k = 1, \ldots, K$, where $\mathcal{S}_k$ is the feasible region corresponding to the kth user's target in (22). By using similar reasoning as in the proof of Theorem 1, we conclude that $\mathcal{S}_k$ and consequently $\mathcal{S}$ are convex sets. Let us construct the procedure for determining the feasibility of a particular vector $\boldsymbol{g} = \bar{\boldsymbol{g}}$ and the separation hyperplane π_k according to (27), with respect to the kth user constraint and the domain $\mathcal{S}_k$ only. Clearly, as illustrated in Fig. 8 for a 3-user system, the global feasibility checking routine would consist of examining each of the user constraints. If, e.g., the kth constraint is declared infeasible, the hyperplane π_k separates $\bar{\boldsymbol{g}}$ and $\mathcal{S}$, as well. $\bar{\boldsymbol{g}}$ is feasible, if and only if each of the K constraints is fulfilled.

First, we rewrite the kth user's constraint in (22) as

$$\left\|\boldsymbol{\Psi}_k(\boldsymbol{g})\boldsymbol{\delta}_k + \boldsymbol{\psi}_k(\boldsymbol{g})\right\|_2 \leq \boldsymbol{\alpha}_k^T(\boldsymbol{g})\boldsymbol{\delta}_k + \beta_k(\boldsymbol{g}), \quad \forall \|\boldsymbol{\delta}_k\|_2 \leq 1, \tag{50}$$

where $\boldsymbol{\delta}_k = \frac{1}{\varepsilon_k}\tilde{\boldsymbol{\Delta}}^T_{(k,:)}$ and $\boldsymbol{\Psi}_k$, $\boldsymbol{\psi}_k$, $\boldsymbol{\alpha}_k$ and β_k are affine in the unknown transmit filter coefficients grouped in the vector $\boldsymbol{g}$. For the constraints of type (50), robust optimization theory, developed in [39], can be applied, in order to examine the feasibility and determine the separation hyperplane. In the sequel, we present the main ideas of the procedure. The user index k and the explicit dependence of the terms $\boldsymbol{\Psi}_k$, $\boldsymbol{\psi}_k$, $\boldsymbol{\alpha}_k$ and β_k on $\boldsymbol{g}$ will be occasionally omitted in rest of this section to make the formulas less cumbersome.

The feasibility problem is resolved by the following lemma:

Lemma 2: The uncertain constraint (50) is valid if and only if the following two inequalities are fulfilled

$$\|\boldsymbol{\alpha}\|_2 \leq \beta, \tag{51}$$

$$\boldsymbol{X}(\lambda) \triangleq \begin{bmatrix} \lambda\boldsymbol{I} + \boldsymbol{\alpha}\boldsymbol{\alpha}^T - \boldsymbol{\Psi}^T\boldsymbol{\Psi} & \beta\boldsymbol{\alpha} - \boldsymbol{\Psi}^T\boldsymbol{\psi} \\ \beta\boldsymbol{\alpha}^T - \boldsymbol{\psi}^T\boldsymbol{\Psi} & \beta^2 - \boldsymbol{\psi}^T\boldsymbol{\psi} - \lambda \end{bmatrix} \succeq \boldsymbol{0}, \tag{52}$$

for some $\lambda \geq 0$. The feasibility of (51)-(52) for a fixed $\boldsymbol{g}$ can be determined in an efficient manner. In the case when (52) is infeasible, a finite set of vectors $\boldsymbol{z}_l$ with the corresponding affine functions $\phi_l(\lambda) = \boldsymbol{z}_l^T\boldsymbol{X}(\lambda)\boldsymbol{z}_l$, $l = 0, \ldots, L$ so that

$$\phi(\lambda) = \min\{\phi_0(\lambda), \ldots, \phi_L(\lambda)\} < 0, \quad \forall\lambda \geq 0, \tag{53}$$

where $\min$ means the pointwise minimum, is readily found.

Proof: It can be noticed that (50) requires

$$\boldsymbol{\alpha}^T(\boldsymbol{g})\boldsymbol{\delta} + \beta(\boldsymbol{g}) \geq 0, \quad \forall\|\boldsymbol{\delta}\|_2 \leq 1. \tag{54}$$

(51) is obtained by applying the Cauchy-Schwarz inequality on (54). Now the inequalities in (50) can be squared, and a direct use of the $\mathcal{S}$-Lemma renders the equivalent form (52).

It is straightforward to examine the validity of (51) for a given vector $\boldsymbol{g} = \bar{\boldsymbol{g}}$, so in the sequel we focus on analyzing (52). For a fixed $\boldsymbol{g}$, $\boldsymbol{X}(\lambda)$ is an LMI in λ. Notice that $\lambda_- \leq \lambda \leq \lambda_+$, where $\lambda_- = 0$, $\lambda_+ = \beta^2 - \boldsymbol{\psi}^T\boldsymbol{\psi}$, must be valid, for (52) to hold. In other words, $[\lambda_-, \lambda_+]$ can be considered as a starting search interval for λ, so that the LMI (52) is positive semidefinite. Therefore, for $\lambda_+ < 0$, it can be immediately concluded that (52) and consequently (50) are not feasible. If $\lambda_+ > 0$, check whether $\boldsymbol{X}(\lambda_l) \succeq \boldsymbol{0}$, with $\lambda_l = 0.5(\lambda_- + \lambda_+)$. If $\boldsymbol{X}(\lambda_l)$ is positive semidefinite, the required λ is λ_l, and the feasibility of (52) can be claimed. If not, by examining the eigenvalues of $\boldsymbol{X}(\lambda_l)$, a vector $\boldsymbol{z}_l$ can be found so that an affine function $\phi_l(\lambda) = \boldsymbol{z}_l^T\boldsymbol{X}(\lambda)\boldsymbol{z}_l$ is negative for $\lambda = \lambda_l$. A new interval $[\lambda_-, \lambda_+]$ to search for λ satisfying $\boldsymbol{X}(\lambda) \succeq \boldsymbol{0}$ is obtained as a set of values for which $\phi_l(\lambda) \geq 0$, and the procedure can be continued in an iterative manner. The new search interval is at least two times smaller than the original search space, which guarantees a rapid convergence [39]. Finally, if no $\lambda \geq 0$ is found so that $\boldsymbol{X}(\lambda) \succeq \boldsymbol{0}$, (52) is declared infeasible, with a set of functions $\phi_l(\lambda)$, that are affine in λ and satisfy (53), obtained. ■

We show now how, when (50) is infeasible, one vector $\bar{\boldsymbol{\delta}}$, with $\|\bar{\boldsymbol{\delta}}\|_2 \leq 1$, can be found so that the first inequality in (50) is not satisfied for $\boldsymbol{\delta} = \bar{\boldsymbol{\delta}}$. Using this infeasibility certificate vector, we will construct the separating hyperplane (27).

In the case when (51) is infeasible, the required vector $\bar{\boldsymbol{\delta}}$ is easily obtained as $\bar{\boldsymbol{\delta}} = -\frac{\boldsymbol{\alpha}}{\|\boldsymbol{\alpha}\|_2}$. We focus in the sequel on the problem when the infeasibility of (51)-(52) is due to (52).

It can be noticed that the obtained $\phi(\lambda)$ in (53) is a piecewise linear concave function for $\lambda \geq 0$. Observe its maximum, and conclude that an $x \in (0, 1)$ and $0 \leq l_1, l_2 \leq L$ can be found so that (the procedure should be slightly modified if one affine function is the minimizer of ϕ for all $\lambda \geq 0$)

$$\varphi(\lambda) = x\phi_{l_1}(\lambda) + (1 - x)\phi_{l_2}(\lambda) < 0, \quad \forall\lambda \geq 0. \tag{55}$$

Set $\boldsymbol{\mu} = \sqrt{x}\boldsymbol{z}_{l_1}$, $\boldsymbol{\zeta} = \sqrt{1-x}\boldsymbol{z}_{l_2}$ and $\boldsymbol{Z} = \boldsymbol{\mu}\boldsymbol{\mu}^T + \boldsymbol{\zeta}\boldsymbol{\zeta}^T$. It follows that

$$\varphi(\lambda) = \mathrm{Tr}\{\boldsymbol{X}(\lambda)\boldsymbol{Z}\} < 0, \quad \forall\lambda \geq 0. \tag{56}$$

By using basic linear algebra and the theory of quadratic functions, it can be shown that a transformation $\boldsymbol{Z} = \boldsymbol{\eta}\boldsymbol{\eta}^T + \boldsymbol{\xi}\boldsymbol{\xi}^T$, where $\boldsymbol{\eta}$, $\boldsymbol{\xi}$ are elements of the second-order cone $\mathbb{L}^{2M+1}$ [32], can be calculated [39]. From (56), one concludes that $\mathrm{Tr}\{\boldsymbol{Z}\boldsymbol{X}(0)\} < 0$. It follows that either $\mathrm{Tr}\{\boldsymbol{\eta}\boldsymbol{\eta}^T\boldsymbol{X}(0)\} < 0$, or $\mathrm{Tr}\{\boldsymbol{\xi}\boldsymbol{\xi}^T\boldsymbol{X}(0)\} < 0$, or both. If the first inequality is true, the required infeasibility certificate $\bar{\boldsymbol{\delta}}$ is obtained by scaling $\boldsymbol{\eta}$ with its last element: $\begin{bmatrix} \bar{\boldsymbol{\delta}}^T & 1 \end{bmatrix}^T = \frac{1}{\eta_{2M+1}}\boldsymbol{\eta}$. The proof follows from the facts that $\begin{bmatrix} \bar{\boldsymbol{\delta}}^T & 1 \end{bmatrix} \boldsymbol{X}(0) \begin{bmatrix} \bar{\boldsymbol{\delta}}^T & 1 \end{bmatrix}^T < 0$ implies that the first inequality in (50) is not valid, and that $\boldsymbol{\eta} \in \mathbb{L}^{2M+1}$ yields $\|\bar{\boldsymbol{\delta}}\|_2 \leq 1$. The analog procedure can be performed when $\mathrm{Tr}\{\boldsymbol{\xi}\boldsymbol{\xi}^T\boldsymbol{X}(0)\} < 0$.

Let $\bar{\boldsymbol{y}} = \begin{bmatrix} (\boldsymbol{\Psi}(\bar{\boldsymbol{g}})\bar{\boldsymbol{\delta}} + \boldsymbol{\psi}(\bar{\boldsymbol{g}}))^T & \boldsymbol{\alpha}^T(\bar{\boldsymbol{g}})\bar{\boldsymbol{\delta}} + \beta(\bar{\boldsymbol{g}}) \end{bmatrix}^T \notin \mathbb{L}^{2K+2}$. Set

$$\boldsymbol{v} = \begin{bmatrix} (\boldsymbol{\Psi}(\bar{\boldsymbol{g}})\bar{\boldsymbol{\delta}} + \boldsymbol{\psi}(\bar{\boldsymbol{g}}))^T \left\|\boldsymbol{\Psi}(\bar{\boldsymbol{g}})\bar{\boldsymbol{\delta}} + \boldsymbol{\psi}(\bar{\boldsymbol{g}})\right\|_2^{-1} & -1 \end{bmatrix}^T. \tag{57}$$

It can be noticed that $\boldsymbol{v}^T\bar{\boldsymbol{y}} \geq \boldsymbol{v}^T\boldsymbol{y}$, for all $\boldsymbol{y} \in \mathbb{L}^{2K+2}$. The homogenous part of

$$\boldsymbol{v}^T \begin{bmatrix} (\boldsymbol{\Psi}(\boldsymbol{g})\bar{\boldsymbol{\delta}} + \boldsymbol{\psi}(\boldsymbol{g}))^T & \boldsymbol{\alpha}^T(\boldsymbol{g})\bar{\boldsymbol{\delta}} + \beta(\boldsymbol{g}) \end{bmatrix}^T, \tag{58}$$

which is immediately computed because of the affine nature of the respective terms in $\boldsymbol{g}$, yields the required vector $\boldsymbol{a}_t$.

The fact that the described ellipsoid method converges to the optimal solution with a polynomial complexity follows directly from Lecture 5 in [29].

REFERENCES

[1] S. N. Diggavi, N. Al-Dhahir, A. Stamoulis, and A. R. Calderbank, “Great expectations: The value of spatial diversity in wireless networks,” *Proc. IEEE*, vol. 92, no. 2, pp. 219–270, Feb. 2004.

[2] R. F. H. Fischer, *Precoding and Signal Shaping for Digital Transmission*. New York, USA: John Wiley and Sons, Inc., 2002.

[3] B. Hassibi and B. M. Hochwald, “How much training is needed in multiple-antenna wireless links?” *IEEE Trans. Inf. Theory*, vol. 49, no. 4, pp. 951–963, Apr. 2003.

[4] D. J. Love, R. W. Heath Jr., W. Santipach, and M. L. Honig, “What is the value of limited feedback for MIMO channels?” *IEEE Comm. Mag.*, vol. 42, pp. 54–59, Oct. 2004.

[5] N. Jindal, “MIMO broadcast channels with finite-rate feedback,” *IEEE Trans. Inf. Theory*, vol. 52, no. 11, pp. 5045–5060, Nov. 2006.

[6] G. Jöngren, M. Skolgund, and B. Ottersten, “Combining beamforming and orthogonal space-time block coding,” *IEEE Trans. Inf. Theory*, vol. 48, no. 3, pp. 611–627, Mar. 2002.

[7] T. Weber, A. Sklavos, and M. Meurer, “Imperfect channel-state information in MIMO transmission,” *IEEE Trans. Commun.*, vol. 54, no. 3, pp. 543–552, Mar. 2006.

[8] Y. Rong, S. A. Vorobyov, and A. B. Gershman, "Robust linear receivers for multi-access space-time block coded MIMO systems: A probabilistically constrained approach," *IEEE J. Sel. Areas Commun.*, vol. 24, no. 8, pp. 1560–1570, Aug. 2006.

[9] M. Botros Shenouda and T. N. Davidson, "Tomlinson-Harashima precoding for broadcast channels with uncertainty," *IEEE J. Sel. Areas Commun.*, vol. 25, pp. 1380–1389, Sep. 2007.

[10] ——, "On the design of linear transceivers for multiuser systems with channel uncertainty," *IEEE J. Sel. Areas Commun.*, vol. 26, no. 6, pp. 1015–1024, Aug. 2008.

[11] X. Zhang, D. P. Palomar, and B. Ottersten, "Statistically robust design of linear MIMO transceivers," *IEEE Trans. Signal Process.*, vol. 56, no. 8, pp. 3678–3689, Aug. 2008.

[12] S. Zhou and G. B. Giannakis, "Optimal transmitter eigen-beamforming and space-time block coding based on channel mean feedback," *IEEE Trans. Signal Process.*, vol. 50, no. 10, pp. 2599–2613, Oct. 2002.

[13] S. A. Jafar and A. Goldsmith, "Transmitter optimization and optimality of beamforming for multiple antenna systems with imperfect feedback," *IEEE Trans. Wireless Commun.*, vol. 3, no. 4, pp. 1165–1175, Jul. 2004.

[14] S. A. Kassam and H. V. Poor, "Robust techniques for signal processing: A survey," *Proc. of the IEEE*, vol. 73, no. 3, pp. 433–482, Mar. 1985.

[15] S. A. Vorobyov, A. B. Gershman, and Z.-Q. Luo, "Robust adaptive beamforming using worst-case performance optimization: A solution to the signal mismatch problem," *IEEE Trans. Signal Process.*, vol. 51, no. 2, pp. 313–324, Feb. 2003.

[16] Y. C. Eldar and N. Merhav, "A competitive minimax approach to robust estimation of random parameters," *IEEE Trans. Signal Process.*, vol. 52, no. 7, pp. 1931–1946, Jul. 2004.

[17] R. Lorenz and S. P. Boyd, "Robust minimum variance beamforming," *IEEE Trans. Signal Process.*, vol. 53, no. 5, pp. 1684–1696, May 2005.

[18] A. Pascual-Iserte, D. P. Palomar, A. I. Perez-Neira, and M. A. Lagunas, "A robust maximin approach for MIMO communications with imperfect channel state information based on convex optimization," *IEEE Trans. Signal Process.*, vol. 54, no. 1, pp. 346–360, Jan. 2006.

[19] Y. Guo and B. C. Levy, "Robust MSE equalizer design for MIMO communication systems in the presence of model uncertainties," *IEEE Trans. Signal Process.*, vol. 54, no. 5, pp. 1840–1852, May 2006.

[20] A. Wiesel, Y. C. Eldar, and S. Shamai, "Optimization of the MIMO compound capacity," *IEEE Trans. Wireless Commun.*, vol. 6, no. 3, pp. 1094–1101, Mar. 2007.

[21] M. Bengtsson and B. Ottersten, "Optimum and suboptimum transmit beamforming," in *Handbook of Antennas in Wireless Communications*, L. C. Godara, Ed. FL, USA: CRC Press, 2002.

[22] M. Schubert and H. Boche, "Solution of the multi-user downlink beamforming problem with individual SINR constraints," *IEEE Trans. Veh. Technol.*, vol. 53, pp. 18–28, Jan. 2004.

[23] S. Shi and M. Schubert, "MMSE transmit optimization for multi-user multi-antenna systems," in *Proc. ICASSP 2005*, Philadelphia, USA, Mar. 2005.

[24] A. Wiesel, Y. C. Eldar, and S. Shamai, "Linear precoding via conic optimization for fixed MIMO receivers," *IEEE Trans. Signal Process.*, vol. 54, no. 1, pp. 161–176, Jan. 2006.

[25] D. P. Palomar and Y. Jiang, "MIMO transceiver design via majorization theory," in *Foundations and Trends in Communications and Information Theory*, S. Verdu, Ed. Hanover, USA: Now publishers, 2006.

[26] M. Payaró, A. Pascual-Iserte, and M. Á. Lagunas, "Robust power allocation designs for multiuser and multiantenna downlink communication systems through convex optimization," *IEEE J. Sel. Areas Commun.*, vol. 25, no. 7, pp. 1390–1401, Sep. 2007.

[27] M. Botros Shenouda and T. N. Davidson, "Convex conic formulations of robust downlink precoder design with quality of service constraints," *IEEE J. Sel. Topics Signal Process.*, vol. 1, no. 4, pp. 714–724, Dec. 2007.

[28] L. Vandenberghe and S. Boyd, "Semidefinite programming," *SIAM Review*, vol. 38, pp. 49–95, Mar. 1996.

[29] A. Ben-Tal and A. Nemirovski, *Lectures on modern convex optimization: Analysis, Algorithms, and Engineering Applications*. PA, USA: MPS-SIAM Series on Optimization, 2001.

[30] M. Botros Shenouda and T. N. Davidson, "Design of fair multi-user transceivers with QoS and imperfect CSI," in *Proc. Communication Networks and Services Research Conference*, Halifax, Canada, May 2008.

[31] ——, "Non-linear and linear broadcasting with QoS requirements: Tractable approaches for bounded channel uncertainties," submitted for publication in IEEE Trans. Signal Process., available online: http://arxiv.org/abs/0712.1659.

[32] S. Boyd and L. Vandenberghe, *Convex Optimization*. NY, USA: Cambridge University Press, 2004.

[33] R. A. Horn and C. R. Johnson, *Matrix Analysis*. NY, USA: Cambridge University Press, 1999.

[34] N. D. Sidiropoulos, T. N. Davidson, and Z.-Q. Luo, "Transmit beamforming for physical layer multicasting," *IEEE Trans. Signal Process.*, vol. 54, no. 6, pp. 2239–2251, Jun. 2006.

[35] A. Goldsmith, *Wireless Communications*. New York, NY, USA: Cambridge University Press, 2005.

[36] N. Vucic and H. Boche, "Robust minimax equalization of imperfectly known frequency selective MIMO channels," in *Proc. Asilomar 2007*, Pacific Grove, CA, USA, Nov. 2007.

[37] I. Pólik and T. Terlaky, "A survey of the S-lemma," *SIAM Review*, vol. 49, 2007.

[38] Z.-Q. Luo and W. Yu, "An introduction to convex optimization for communications and signal processing," *IEEE J. Sel. Areas Commun.*, vol. 24, no. 8, pp. 1426–1438, Aug. 2006.

[39] A. Ben-Tal, D. Bertsimas, L. E. Ghaoui, A. Nemirovski, and M. Sim, "Robust Optimization," in preparation, available online: http://iew3.technion.ac.il/∼nemirovs/index.html.

[40] A. Mutapcic, S.-J. Kim, and S. Boyd, "A tractable method for robust downlink beamforming in wireless communications," in *Proc. Asilomar 2007*, Pacific Grove, CA, USA, Nov. 2007.

[41] J. F. Sturm, "Using SeDuMi 1.02, a MATLAB tool for optimization over symmetric cones," in *Optimization Methods and Software*, vol. 11-12, 1999, pp. 625–653.

[42] N. Vucic, H. Boche, and S. Shi, "Robust MSE-constrained downlink precoding in multiuser MIMO systems with channel uncertainty," in *Proc. Allerton 2007*, Monticello, IL, USA, Sep. 2007.

Nikola Vučić (S'06) received the Dipl.-Ing. degree in electrical engineering from the University of Belgrade, Serbia, in 2002. He is currently pursuing the Ph.D. degree in electrical engineering with the Technical University of Berlin, Germany.

Since 2003, he has been with the Fraunhofer Institute for Telecommunications - Heinrich Hertz Institute, Berlin, Germany. His research interests include transceiver design for multi-antenna systems and robust optimization.

Holger Boche (M'04 - SM'07) received his Dipl.-Ing. and Dr.-Ing. degrees in electrical engineering from the Technische Universität Dresden, Germany, in 1990 and 1994, respectively. In 1992, he graduated in mathematics from the Technische Universität Dresden, and in 1998 he received his Dr.rer.nat. degree in pure mathematics from the Technische Universität Berlin, Germany.

From 1994 to 1997, he did postgraduate studies in mathematics at the Friedrich-Schiller Universität Jena, Germany. In 1997, he joined the Heinrich-Hertz-Institut (HHI) für Nachrichtentechnik Berlin. He is head of the Broadband Mobile Communication Networks department at HHI. Since 2002, he is Full Professor for Mobile Communication Networks at the Technische Universität Berlin, Institute for Communication Systems, and since 2003 he is director of the Fraunhofer German-Sino Lab for Mobile Communications, Berlin, Germany. He was visiting professor at the ETH Zurich during winter term 2004 and 2006, and at KTH Stockholm during summer term 2005. Prof. Boche received the Research Award "Technische Kommunikation" from the Alcatel SEL Foundation in October 2003, the "Innovation Award" from the Vodafone Foundation in June 2006, and Gottfried Wilhelm Leibniz Prize from the German Research Foundation DFG in 2008. He was co-recipient of the 2006 IEEE Signal Processing Society Best Paper Award and recipient of the 2007 IEEE Signal Processing Society Best Paper Award. He is a member of IEEE Signal Processing Society SPCOM and SPTM Technical Committee. He was elected a member of the German Academy of Sciences (Leopoldina) in 2008.